Photonic Microwave Arbitrary Waveform Generation Using a Virtually Imaged Phased-Array (VIPA) Direct Space-to-Time Pulse Shaper

Shijun Xiao, *Student Member, IEEE*, Jason D. McKinney, *Member, IEEE*, and Andrew M. Weiner, *Fellow, IEEE*

***Abstract*—We present the first direct space-to-time pulse shaper using a virtually imaged phased array as the spectral disperser. We use this pulse shaper to demonstrate generation of 10–50-GHz arbitrary microwave waveforms with time apertures as large as 1.0 ns and peak-to-peak amplitudes as high as 400 mV.**

***Index Terms*—Optical pulse shaping, optical spectral disperser, photonic arbitrary waveform generation, radio-frequency (RF) photonics.**

PHOTONIC microwave arbitrary waveform generation is a new research area with potential applications in radio-frequency (RF)/microwave communication systems such as ultrawide-band and multiple-access communication systems as well as in pulsed radar and electronic countermeasures. In previous work, a diffraction grating-based direct space-to-time (DST) pulse shaper was used to generate optical pulse trains that excited a high-speed photodiode, resulting in 20–50-GHz millimeter waveforms with $\sim$100-ps temporal apertures and with $\sim$20-mV amplitudes [1], [2]. Spectral shaping of a supercontinuum source using a Fourier transform pulse shaper and subsequent wavelength-to-time mapping has also been used to generate 1–12-GHz waveforms of $\sim$15-mV peak-to-peak amplitude [3]. Waveforms in the 12.4–37.2-GHz range have also been generated by beating different longitudinal modes of a mode-locked external cavity semiconductor laser selected through a wavelength-division-multiplexing (WDM) technique [4]. Here we demonstrate, for the first time to our knowledge, photonic microwave arbitrary waveform generation using a DST pulse shaper based on a virtually imaged phased-array (VIPA) spectral disperser. Our experiments yield waveforms in the 10–50-GHz range with temporal apertures up to 1.0 ns and peak-to-peak amplitudes up to $\sim$400 mV, which are substantially enhanced compared to previous results.

Fig. 1 shows our experimental setup. We use a passively mode-locked fiber laser, which provides 70-fs pulses at 50-MHz repetition rate around 1.55 um. After propagation in a single-mode fiber link and amplification in an erbium-doped fiber amplifier (EDFA), the input pulse is broadened to $\sim$1 ps prior to coupling into the VIPA-based DST pulse shaper. We use a solid VIPA provided by the Avanex Corporation with a 50-GHz FSR. The output light from the pulse shaper is coupled into a single-mode fiber and amplified by another EDFA. The output optical signal is either measured using an optical cross correlator or used to drive a fast photodiode for microwave arbitrary waveform generation. In the latter scenario, the photodiode output is measured on a 50-GHz sampling oscilloscope. The remainder of this letter is structured as follows. We will first discuss the DST pulse shaper based on the VIPA, and we will then discuss use of this apparatus for optical pulse sequence and microwave waveform generation.

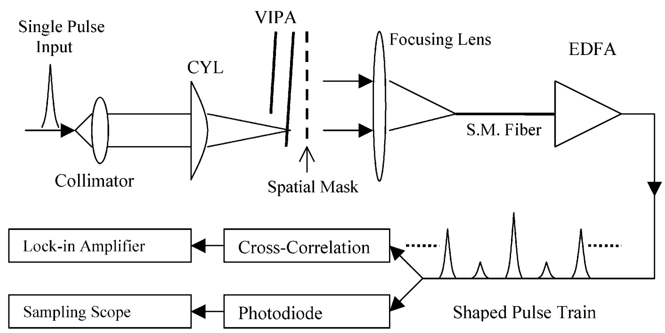

Fig. 1. VIPA-DST pulse shaper setup used for photonic arbitrary waveform generation. Two photodiodes with 60- and 20-GHz bandwidths, respectively, are used for O/E conversion at the output. Waveforms are measured with a 50-GHz sampling oscilloscope. CYL: cylindrical lens.

The VIPA is a relatively new optical spectral disperser based on a "side-entrance" Fabry–Pérot etalon geometry [5]. It typically consists of two glass plates, of which the back or the transmission side is coated with a partially reflective film (e.g., $\geq$95%); the front or entry side is coated with an almost 100% reflective film except in a window area, which is uncoated or antireflection coated. A collimated beam is focused by a cylindrical lens into the VIPA at a small angle through the window area, and the injected beam experiences multiple reflections between two plates of the VIPA. The angular dispersion is achieved via multiple beam interference. An important property of the VIPA is that it can provide significantly larger angular dispersion than typical diffraction gratings, and recently, we have constructed an analytical theory for the dispersion law of the VIPA [6]. One important application of the VIPA is in demultiplexing–multiplexing for WDM systems, and we have demonstrated demultiplexing with -3-dB channel bandwidths as small as 1 GHz [7], which makes the VIPA appealing for potential applications in hyperfine WDM.

Another new application of the VIPA, demonstrated here for the first time to our knowledge, is in DST pulse shaping [8], [9]. Fundamentally different from the well-established Fourier transform pulse shaper [10], the temporal output of the

Manuscript received March 5, 2004; revised May 3, 2004. This work was supported in part by the ARO under Grant DAAD19-03-1-0275 and by the NSF under Grant 0 100 949-ECS.

The authors are with the School of Electrical and Computer Engineering, Purdue University, West Lafayette, IN 47907-1285, USA (e-mail: sxiao@ecn.purdue.edu; mckinnjd@ecn.purdue.edu; amw@ecn.purdue.edu).

Digital Object Identifier 10.1109/LPT.2004.831324

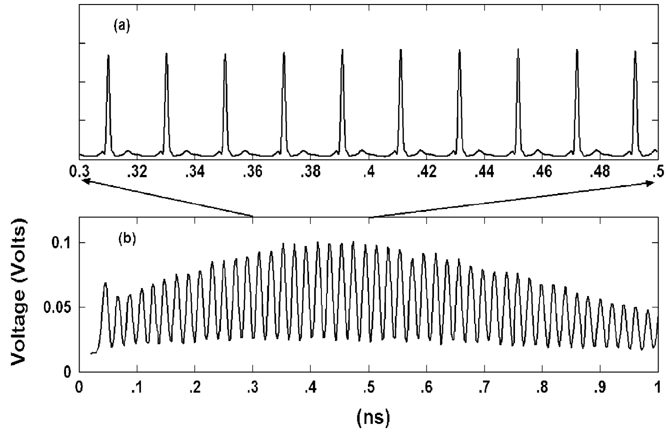

Fig. 2. (a) Output optical pulse sequence due to a single pulse input into the 50-GHz solid VIPA. (b) The 50-GHz microwave tone burst measured after O/E conversion using a 60-GHz photodiode. (a) Optical pulse train. (b) RF waveform.

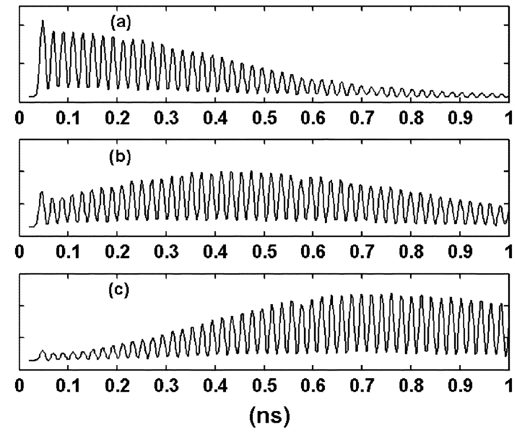

Fig. 3. Waveforms exhibiting different temporal windows. Control is achieved by tuning the angle of the output single-mode fiber. The 60-GHz photodiode is used. (a) Single sided exponential. (b) Gaussian-like. (c) Shifted Gaussian-like.

DST pulse shaper when read-out by an ultrashort pulse is a directly scaled version of the input spatial masking function. Unlike the previously demonstrated grating-based DST pulse shapers [8], [9], multiple reflections within the VIPA lead to an array of spots on the VIPA output surface, which acts as an intrinsic spatial masking pattern with a decaying exponential profile. Similar to the short pulse response of arrayed-waveguide gratings [11], the multiple delay paths associated with the multiple reflections in the VIPA lead to a series of output pulses with a repetition rate equal to the VIPAs free spectral range (FSR). The duration of an individual output pulse is determined by the input pulsewidth, while the duration of the envelope of the output pulse burst varies inversely with the -3-dB bandwidth of the VIPA demultiplexer. The narrow -3-dB bandwidth ($\sim$1 GHz) of the VIPA leads to a temporal window up to 1 ns, approximately an order of magnitude higher than previously demonstrated with a grating-based DST pulse shaper [1], [2]. A 200-ps portion (determined by the effective scan range of our cross correlator) of a typical optical pulse sequence obtained from the VIPA DST is illustrated in Fig. 2(a). In our cross-correlation measurement, the reference laser beam from the fiber laser maintains the 70-fs duration. The side lobes in the cross-correlation trace are attributed to nonideal effects such as unexpected reflections; however, these are not important as we are interested in photonic waveform generation. We use the output optical pulse sequences from our VIPA-based DST pulse shaper to drive either a 60- or 20-GHz photodiode for microwave waveform generation. Here, the photodiode serves as a low pass filter for our optical pulse sequences. Therefore, the speed of the photodiode is selected based on the frequency content of the desired waveform. For example, when the periodic 50-GHz pulse train of Fig. 2(a) is used to drive the 60-GHz optical-to-electrical (O/E) converter, the result is a 50-GHz tone burst shown in Fig. 2(b). Here, the 1-ns temporal aperture is obviously demonstrated by the measured electrical waveform resulting from this high-speed O/E conversion, and this results in $\sim$1-GHz -3-dB spectral bandwidth (calculated). By tailoring the center frequency of our microwave signals relative to the $\sim$1-ns temporal window, signals with large fractional bandwidths maybe obtained—an attractive capability for applications in ultrawide-band communication systems. In addition, an interesting point is that the finite acceptance angle of the single-mode fiber used as the system output can be used to select different portions of the optical pulse sequence from the VIPA output surface. The multiple output beams from the VIPA are focused into the fiber at different angles, and this can result in a shift of the temporal window as different coupling angles yield different coupling efficiency for the different output beams. When the temporal window peak is chosen appropriately, the total effect due to the temporal window and the exponential window associated with the VIPA beam profile is a smooth Gaussian-like temporal window. By tuning the fiber angle, we demonstrate control of the temporal windows of our waveforms: Fig. 3(a) shows a single-sided exponentially decaying waveform, and this illustrates the expected exponentially decaying optical pulse train from the VIPA-based DST pulse shaper. Fig. 3(b) shows a waveform with a Gaussian-like time aperture. Fig. 3(c) shows a shifted Gaussian-like time aperture waveform, which has been truncated at $t = 1$ ns due to the oscilloscope sampling range.

Additional control over the optical pulse sequence from the pulse shaper is achieved by inserting a spatially patterned mask directly after the VIPA output surface. In grating-based DST pulse shapers, the temporal output in response to an ultrashort pulse input is a directly scaled version of the applied spatial masking pattern. For the VIPA DST pulse shaper, the mask modulates different pulses in the intrinsic periodic output train. Therefore, the output is a scaled version of the masking function multiplied by the intrinsic output pulse sequence. Our spatial masks are made from transparent film printed with a series of black bars, which function as spatially patterned amplitude control elements. Programmable control could be possible by using a spatial light modulator (SLM) similar to those that are widely used in Fourier transform pulse shaping [10]. Here, we use a 20-GHz O/E converter. With a periodic amplitude mask designed to select every Nth spot on the VIPA transmission side, the repetition rate of the output pulse sequence is reduced to (FSR/N). Fig. 4(a) shows a 16.7-GHz waveform generated in this manner. Here the pulse repetition rate is reduced to FSR/3 as is clearly shown in the optical pulse sequence

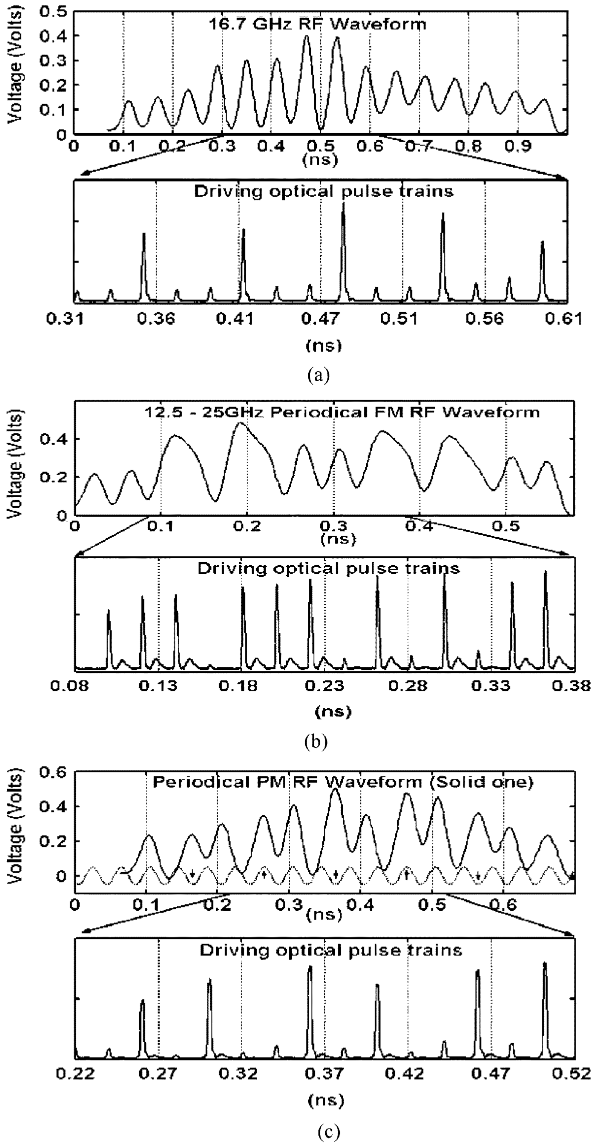

Fig. 4. Large temporal window and high amplitude arbitrary waveforms generated using a solid VIPA with 50-GHz FSR and a 20-GHz photodiode. (a) 16.7-GHz tone burst, (b) 12.5–25-GHz wide-band FM, and (c) wide-band PM. The dashed line in (c) is a software-generated sinusoid that provides a reference for visualization of the PM.

(bottom trace). The low-amplitude residual optical pulses are effectively filtered by the 20-GHz bandwidth of the photodiode. Arbitrary electrical waveforms and driving pulse trains can be obtained using more complex mask patterns. For convenience, we denote the spots at the VIPA output with index $\{1, 2, 3, \ldots\}$ starting from the first incident spot. When we use a mask to select spots $\{1, 3, 5, 6, 7, 9, 10, 11, \ldots\}$ (the mask repeats every 12 spots), we generate an abruptly frequency-modulated (FM) waveform that alternates between two 25-GHz cycles and two 12.5-GHz cycles shown in Fig. 4(b). If instead we use a mask to select spots $\{1, 4, 6, 9, \ldots\}$ (the mask repeats every ten spots), we generate a waveform with abrupt, phase modulation (PM), shown in Fig. 4(c). In Fig. 4, the temporal aperture of our waveforms is smaller than the 1-ns aperture of the 50-GHz tone burst [Fig. 2(b)] as we use larger incident angles into the VIPA, which leads to a smaller number of reflections in the VIPA etalon for a fixed VIPA etalon transverse aperture. One nonideal effect apparent in the cross correlations of Fig. 4(a)–(c) is the residual pulses that remain between the pulses used for waveform generation. This is due to the fact that fixed-dimension square amplitude masks cannot totally block diverging Gaussian beams as these beams overlap partially in space just after the VIPA. This leads to weak residual output spots and, hence, weak residual output pulses according to the DST mapping of the DST pulse shaping apparatus. In the case of photonic microwave waveform generation, where shaped pulse trains are used to drive a photodiode, these residual pulses are of no consequence and smooth waveforms are obtained given the low pass filtering effect of the electrical measurement. An important point is that the maximum peak-to-peak amplitude of our microwave waveforms is $\sim$400 mV, which is 20–30 times higher than previously reported [1]–[4]. The voltage amplitude is currently limited by the maximum operating voltage of our fast photodiodes, not by the available optical power. We attribute this improvement to the relatively high optical throughput of the VIPA-based DST pulse shaper.

In summary, we have demonstrated the first direct DST pulse shaper based on the VIPA spectral disperser. We also demonstrate use of the VIPA-DST pulse shaper for photonic microwave arbitrary waveform generation in the range 10–50 GHz with signals exhibiting time apertures as large as 1 ns and signal amplitudes as high as 400 mV.

ACKNOWLEDGMENT

The authors would like to thank C. Lin from the Avanex Corporation for providing the VIPA samples.

REFERENCES

[1] J. D. McKinney, D. E. Leaird, and A. M. Weiner, "Millimeter-wave arbitrary waveform generation with a direct space-to-time pulse shaper," *Opt. Lett.*, vol. 27, no. 15, pp. 1345–1347, 2002.

[2] J. D. McKinney, D. S. Seo, and A. M. Weiner, "Photonically assisted generation of continuous arbitrary millimeter electromagnetic waveforms," *Electron. Lett.*, vol. 39, no. 3, pp. 309–311, 2003.

[3] J. Chou, Y. Han, and B. Jalai, "Adaptive rf-photonic arbitrary waveform generator," *IEEE Photon. Technol. Lett.*, vol. 15, pp. 581–583, Apr. 2003.

[4] T. Yilmaz, C. M. DePriest, T. Turpin, J. H. Abeles, and P. J. Delfyett, "Toward a photonic arbitrary waveform generator using a modelocked external cavity semiconductor laser," *IEEE Photon. Technol. Lett.*, vol. 14, pp. 1608–1610, Nov. 2002.

[5] M. Shirasaki, "Large angular dispersion by a virtually imaged phased array and its application to a wavelength demultiplexer," *Opt. Lett.*, vol. 21, pp. 366–368, May 1996.

[6] S. Xiao, A. M. Weiner, and C. Lin, "A dispersion law for virtually-imaged phased-array (VIPA) spectral dispersers based on paraxial wave theory," *IEEE J. Quantum Electron.*, vol. 40, pp. 420–426, Apr. 2004.

[7] ——, "Demultiplexers with 10 pm (1.25 GHz) −3 dB transmission bandwidth using a virtually imaged phased array (VIPA)," in *Optical Fiber Communication Conf. (OFC)*, Los Angeles, CA, Feb. 22–27, 2004, Paper TuL1.

[8] D. E. Leaird and A. M. Weiner, "Femtosecond direct space-to-time pulse shaping," *IEEE J. Quantum Electron.*, vol. 37, pp. 494–504, Apr. 2001.

[9] J. D. McKinney, D. Seo, and A. M. Weiner, "Direct space-to-time pulse shaping at 1.5 um," *IEEE J. Quantum Electron.*, vol. 39, pp. 1635–1644, Dec. 2003.

[10] A. M. Weiner, "Femtosecond pulse shaping using spatial light modulators," *Rev. Sci. Instrum.*, vol. 71, no. 5, pp. 1929–1960, 2000.

[11] D. E. Leaird, S. Shen, A. M. Weiner, A. Sugita, S. Kamei, M. Ishii, and K. Okamoto, "Generation of high-repetition-rate WDM pulse trains from an arrayed-waveguide grating," *IEEE Photon. Technol. Lett.*, vol. 13, pp. 221–223, Mar. 2001.